



Correlation of anisotropic cell behaviors with topographic aspect ratio

Adam S. Crouch^a, D. Miller^b, Kevin J. Luebke^b, W. Hu^{a,*}

^a Department of Electrical Engineering, University of Texas at Dallas, Richardson, TX 75080, United States

^b Department of Internal Medicine, Division of Translational Research, University of Texas Southwestern Medical Center, Dallas, TX 75390-9185, United States

ARTICLE INFO

Article history:

Received 18 September 2008

Accepted 27 November 2008

Available online 31 December 2008

Keywords:

Nanoimprint lithography

Topography

Aspect ratio

Human dermal fibroblast

Cell alignment

Cell elongation

ABSTRACT

In this study, we have used nanoimprinting to create a range of micro- and nanoscale gratings, or their combination, in bulk polystyrene plates to investigate anisotropic cell behaviors of human dermal fibroblasts with respect to the aspect ratio (depth/width) of gratings. The depth and width of the polystyrene gratings both show strong effects individually on cell alignment and elongation that are qualitatively similar to the results of other studies. However, consistent quantitative comparison of these individual parameters with different studies is complicated by the diversity of combinations of width and depth that have been tested. Instead, the aspect ratio of the gratings as a unified description of grating topography is a more consistent parameter to interpret topographic dependence of cell morphology. Both cell alignment and elongation increase with increasing aspect ratio, and even a shallow grating (aspect ratio of ~ 0.05) is sufficient to induce 80% cell alignment. Re-plotting data recently published by other groups vs. aspect ratio shows a similar dependence, despite differences in cell types and surface structures. This consistency indicates that aspect ratio is a general factor to characterize cell behaviors. The relationship of cell elongation and alignment with topographic aspect ratio is interpreted in terms of the theory of contact guidance. This model provides simplicity and flexibility in geometry design for devices and materials that interface with cells.

Published by Elsevier Ltd.

1. Introduction

To fully realize the potential applications of guided cell growth on patterned surfaces, it is crucial to obtain a fundamental understanding of cell–substratum interactions and establish accurate models for biological and abiological interfaces that predict cell behaviors. In addition, an understanding of cell–substrate interactions gained from *in vitro* studies on precisely engineered topography can provide insight into the complex interactions occurring between the cell and the natural extracellular matrix (ECM), which is itself a complex structure, consisting of nanopores, fibers, ridges and bands [1]. A variety of studies have been conducted for a wide range of cell types displaying changes in cell morphology and function in response to topographic and chemical cues [2–14]. Many patterning methods have also been developed to create microscale and nanoscale structures of different shapes on the surfaces of various materials. The interdisciplinary nature of research in this field has led to extensive understanding of how cells respond to topographic, chemical, mechanical, biological, and even electrical cues. Comprehensive summaries can be found in

several excellent review articles [15–17]. Many of the studies in this area have quantified the anisotropic behaviors, e.g. alignment and elongation, of various cell types on grating structures of varying linewidths or depths [3,5–7,9,13,14,16], an effect related to contact guidance [15,18,19]. These studies have established that almost all types of cells can grow and elongate along the grating direction; both the width and depth/height of gratings (grooves or ridges) can have strong effects on cell behavior. However, the findings of these studies have not been consistent on the degree of such effects. For instance, there were conflicting observations on which property has a stronger effect on cell behavior, e.g. depth or width [16] and nano- or microstructures [3,9,20]. Such inconsistency in cell studies is in part due to the biological complexity associated with using different cell types and more importantly a lack of standard rules for topographic design and control. Many studies have varied one dimension, width or depth, while maintaining poor control over the other or in some cases, ignoring one dimension entirely. Such practices have often led to inaccuracy in predicting cell behavior due to inconclusive data produced by a very limited amount of width–depth variations.

Beyond the empirical relationships observed for particular gratings and cell types in these studies, it would be highly desirable to have general physical models that relate cell interactions to three-dimensional substrate topography. A few recent studies have

* Corresponding author. Tel.: +1 972 883 6329.

E-mail address: walter.hu@utdallas.edu (W. Hu).

used surface roughness, either random roughness or calculated from both pitch and depth of gratings and pillars/pores, to study cell behaviors [21–24]. Roughness, as a combination of width and depth effects, has indeed proven to be a useful factor for describing cell behaviors. Noting a correlation of anisotropic roughness with cell behavior, Lenhart et al. have proposed a capillary force-induced mechanism extended from contact guidance [24]. The observation of linear dependence of cell alignment and elongation on capillary forces related to surface roughness, while interesting and useful, does not lend itself to an intuitive physical picture with which to correlate the shape and dimensions of topography to cell behaviors. Roughness describes lateral topographic variation in two directions, *X*- and *Y*-, which does not facilitate description of anisotropic cell behaviors such as alignment and elongation in only one direction. A recent study has shown that, for similar surface roughness, cells respond quite differently to ordered (aligned grooves) and disordered/random features [23]. Even ordered surfaces, pillars and gratings, show different effects on cells despite having similar surface roughness. In this study, we have studied the anisotropic behaviors of cells adhering to well-controlled gratings of varying widths and depths, aiming to develop a unified factor that describes topographic effects on cell behaviors. Because the gratings impose no constraints on cells along the grating direction, the topographic effect is limited to the spatial constraints on cell spreading in the lateral direction perpendicular to the grating direction. We find that the aspect ratio of the gratings, defined as depth or height over width, is a useful unifying factor to characterize topographic effects on cell alignment and elongation. Although the designs of previously reported experiments have incidentally varied the aspect ratios of gratings, the relationship between cell behavior and aspect ratio has not been explicitly analyzed. This analysis provides new insight into the interactions of cells with their substrates.

A surface patterning method capable of high precision and accuracy over large areas is required to investigate topographic effects on cell behavior. Until recently, few techniques existed that allowed for precise patterning at the nanoscale, making it impossible to model *in vitro* 3D and nanoscale features similar to authentic ECM. Many lithographic methods, including e-beam lithography, nanoimprint lithography (NIL) and microcontact printing, have been explored to mimic this environment [2–5,7,9,25–27]. Yet, many of these methods fall short due to their small patterning areas, micron resolution limits, slow speeds, and high costs. A variety of chemical and solution-based methods, such as electrospinning and solvent casting, provide large patterning areas with high resolution [28–33], but lack precise control over the feature dimensions and orientation. Many of these methods also offer limited ability to fabricate true 3D structures, which are essential in mimicking the ECM. In contrast, nanoimprint lithography affords high throughput, low cost, high resolution, large patterning areas, and overall process flexibility. Recently, work by Hu et al. [9] utilized a double imprint sequence to create 3D structures consisting of nanostructures embedded within micron lines, illustrating the ability of this technique to create 3D structures with nanoscale precision and resolution. NIL is readily applicable, without polymer spincoating, to tissue culture polystyrene (TCPS), a low cost material that works well as a substrate for many adherent cell types. Because of these advantages, we have used NIL to create various micro- and nanoscale gratings for studies of cell response to topography. Human dermal fibroblasts were tested. Their alignment and elongation were quantified for varying widths and depths and analyzed with respect to the grating aspect ratio. Both cell alignment and elongation increase monotonically with increasing aspect ratio of topography, indicating that the aspect ratio is a useful parameter for characterizing cell response to

substrate topography without distinguishing the effects of width and depth. We also observe that dermal fibroblasts are highly sensitive to features of even a small aspect ratio. For instance, 80% of cells aligned to the gratings of aspect ratio 0.05. To further validate the relevance of aspect ratio, data for cell alignment and elongation previously reported by several groups were re-plotted with respect to the aspect ratio of their grating structures. All results show a similar monotonic dependence, though the slope of this dependence varies for different cell types. A simple model is proposed to explain the relationship between aspect ratio and cell behaviors, observed consistently despite use of different substrate materials and cell types. In addition, 3D samples were fabricated utilizing a novel double imprinting technique. Bulk TCPS samples were imprinted twice using well-controlled imprinting conditions to create 3D structures topographically mimicking the striated profile of collagen fiber, incorporating both micron and nanometer-scale structures. Cell alignment was little affected by the superposition of the nanometer-scale structure, likely due to the depth of the embedded structures being below the threshold of cell sensitivity in the context of the micron-scale structure.

2. Materials and methods

2.1. Scaffold material

From a materials' perspective, the low optical contrast of cells requires a transparent substrate for transmission microscopy. For this reason, previous studies have utilized glass and fused silica, both requiring elaborate and expensive patterning techniques, such as plasma etching and chemical processing [15]. Thin polymer films are often utilized for their biocompatibility and biodegradability, but require underlying substrates for support, limiting their application for tissue engineering [9]. In this study, TCPS was directly imprinted using nanoimprint lithography to create micro- and nanostructures. TCPS is a particularly good choice of material due to its low cost, high availability, visual transparency, and support of cell viability. Rigorous studies conducted with this material show the versatility and practicality of TCPS [9,34]. Additionally, the use of a bulk polymer material is particularly advantageous for roll-to-roll imprinting processes, since no polymer spincoating is required [35,36].

2.2. Mold making

To fabricate the Si grating molds, 1.3 μm of S1813 was first spincoated onto a Si substrate. UV contact photolithography was conducted on a Karl Suss MA6 contact aligner to create lines of 2, 5, and 10 μm widths. Etching was conducted on an Oerlikon Versaline inductively coupled plasma (ICP) etching system. ICP etching systems, characterized by low pressures and high ion densities, are capable of producing highly directional, well-controlled nanoscale and deep Si etching. The etching was conducted using Cl_2 plasma at 5 mTorr, an ICP RF power of 300 W, and a bias RF power of 100 W. Various etching times were used to control the depth of the mold from 100 nm to 1.2 μm . An additional mold consisting of 100 nm wide lines of 100 nm depth was purchased from Nanonex. All molds utilized in this study contain equal line and trench spacing, meaning the pitch is twice the linewidth.

2.3. Nanoimprint lithography (NIL)

Nanoimprint lithography [37] is advantageous for this application due to its high throughput, low cost, high resolution, large patterning areas, and overall process flexibility. Resolution limits have been improving over the last decade, and have recently reached linewidths as small as 5 nm [38]. Additionally, 3D structures have been produced on both the micro- and nanoscale in a wide range of polymers and other materials [9,39,40], demonstrating the material and structural flexibilities of this technique.

The processes of single and double layer direct NIL into bulk polymer materials were presented in our earlier work [9]. A similar process was used in this study, but with optimized demolding temperature to achieve less pattern distortion due to reduced thermal stress. The initial imprint sequence was characterized by heating the material well above its glass transition temperature (T_g). A uniform gas pressure of 5 MPa was applied to force material flow into the hydrophobic mold cavities. The shallowest 100 nm depth molds required less filling time (300 s), while the deepest 1 μm molds required more time (720 s). Vertical demolding can be carried out once the material has been cooled below its T_g . Previous trials suggested that cooling the material to room temperature prior to demolding results in global pattern deformations, attributable to a lateral force on the imprinted gratings due to the thermal expansion difference between the mold and material. To alleviate this problem,

demolding was conducted at 70 °C to reduce the temperature difference between the imprinting and mold release.

A second layer imprint was conducted at 5 MPa and 95 °C, around the T_g of TCPS. A previous study by Buck et al. has revealed that the T_g of polystyrene actually decreases by almost 30 °C near the polymer surface when compared to the bulk [41]. Second imprints were conducted to embed 100 nm wide lines into 5 μ m wide lines. Fig. 1 displays example SEM images of the imprinted structures of 100 nm width and depth lines and also 100 nm wide and 50–60 nm deep nano-gratings embedded on top of 2 μ m wide micro-gratings of 500 nm depth. The patterns are seen to be transferred with good fidelity into the TCPS with nearly no edge deformation. The bottom gratings are deformed minimally, displaying a decrease in height of approximately 90 nm, or 18%. Table 1 lists all sample dimensions used in this study, as examined by SEM and AFM.

2.4. Cell seeding

Human foreskin fibroblasts (HFF CRL 2522, ATCC) were maintained in Dulbecco's modified Eagle Medium (DMEM; Gibco) with 10% heat-inactivated Fetal Bovine Serum (FBS; Sigma). Prior to reaching confluence, the fibroblasts were harvested from monolayer culture with 0.25% trypsin/EDTA (Sigma). Trypsin was neutralized with 10% FBS in DMEM. Substrates were sterilized with 70% ethanol; replicate substrates were placed into a single well of a six-well culture plate. Each well had a surface area of 4.8 cm² and each substrate was approximately 1–1.5 cm². Dermal fibroblasts were seeded onto the substrates at a density of 6300 cells/cm² in DMEM supplemented with 10% FBS. After 24 h, the cells were rinsed with phosphate-buffered saline (PBS) then fixed using 4% paraformaldehyde. The cells were then processed for immunofluorescent staining of actin filaments and nuclei with TRITC-conjugated Phalloidin and DAPI using the actin cytoskeleton and focal adhesion staining kit (part # FAK100, Chemicon International) according to the manufacturer's protocol.

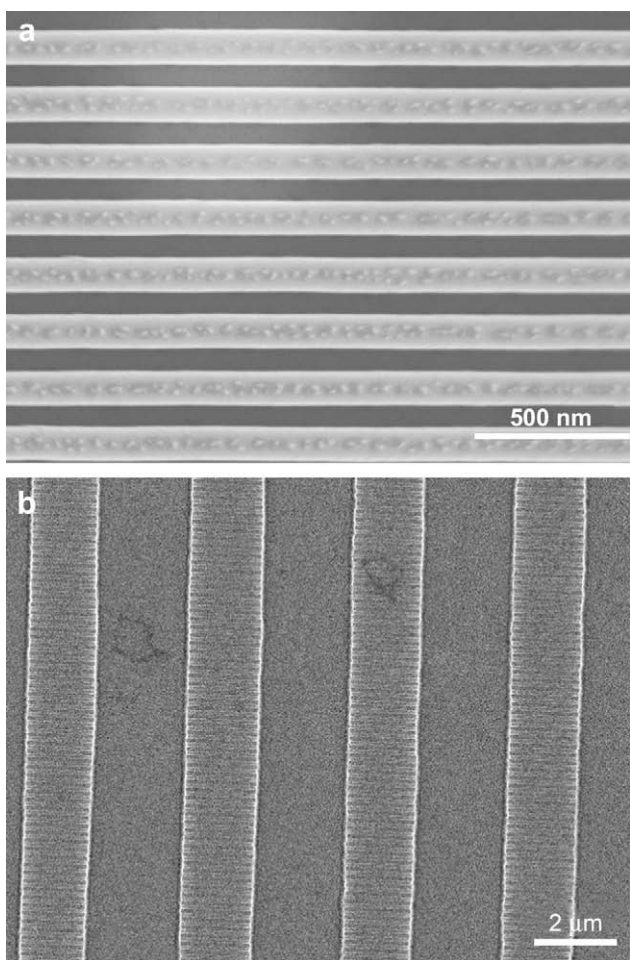


Fig. 1. SEM of (a) 100 nm wide and deep lines of 1:1 line and space ratio in TCPS. The imprint is completed with good fidelity over large areas. (b) 2 μ m lines embedded with 100 nm lines by double imprint at 95 °C and 50 bar.

Table 1

Topographical dimensions of the grating surfaces in TCPS plates, as determined by SEM and AFM.

Sample #	1	2	3	4	5	6	7	8	9	10	11
Aspect ratio	0	0.01	0.02	0.05	0.1	0.16	0.2	0.25	0.4	0.5	1
Width (μ m)	0	10	5	2	5	5	5	2	2	2	0.1
Depth (μ m)	0	0.1	0.1	0.1	0.5	0.8	1	0.5	0.8	1	0.1

2.5. Cell imaging and morphology assessment

Digital microphotographs of fluorescently stained cellular actin, and nuclei were obtained using an Olympus BX51 fluorescent microscope. Digital microphotographs of the cells were also obtained using a light microscope with phase contrast. The light microscope images were used to manually measure the cell alignment of the fibroblasts with respect to the imprinted pattern. The angles between the grating and cell long axis were measured for 20 randomly chosen cells in the patterned area and 20 randomly chosen cells in the non-patterned area of each substrate. Three to five substrates for each imprint pattern were studied. For the cells on gratings, Gaussian distributions centered to the grating direction of the number of cells over the measured angle were observed, indicating good data assessment. To calculate the percentage of cells aligned with the grating, a conventional standard of cell alignment was used, defined as alignment of the cell's long axis within 15° of the grating direction [5,9,13]. SEM was also used in judging alignment on the nanoscale patterns. The elongation factor (long axis/short axis – 1) [6] of the cells was also measured manually on images from the light microscope, similarly measuring 20 randomly chosen cells in the patterned area and 20 randomly chosen cells in the non-patterned area of each substrate for three to five substrates of each pattern.

3. Results

3.1. Alignment on grating structures

The fluorescent images of Fig. 2 display the cells fixed on a variety of substrates. Fig. 2a shows cells on patterned grating and non-patterned polystyrene areas, indicating a significant difference in cell alignment and morphology. Increased alignment was generally observed as the linewidth decreased and the line depth increased. These trends are illustrated in Fig. 2b and Fig. 3a and b, displaying the alignment as a function of linewidth and depth for a variety of samples. A maximum alignment of 97.3% was found to occur for 5 μ m lines with a depth of 800 nm, while a minimum alignment of 60% occurred for 10 μ m lines only 100 nm in depth. Fig. 3c displays the measured alignments as a function of aspect ratio of the grating, which is defined as grating depth over width. As the aspect ratio increases across a variety of grating dimensions, the alignment increases, defining a clear relationship between the cell alignment and aspect ratio. A grating of very small aspect ratio (\sim 0.05) can already significantly affect cell alignment (\sim 85%). An aspect ratio of only 0.16 yields a cell alignment of 97%. Cell alignment appears to saturate at this aspect ratio, remaining fairly consistent around 95% alignment for further increasing aspect ratios. In Table 1, the aspect ratios in Fig. 3 are tabulated with the corresponding widths and depths used in the experiment.

3.2. Cell elongation

The elongation factor (long axis/short axis – 1) was measured for each sample and is shown in Fig. 4a. For increasing aspect ratios, the elongation of the cells generally increased, though the aspect ratios of 0.2 and 0.25 appear to deviate somewhat from this trend. The most dramatic elongation changes occur for aspect ratios from 0.01 to 0.1. The linewidth and depth both have a significant effect on elongation, as illustrated in Fig. 4b and c.

3.3. Alignment on collagen-like 3D structures

Similar alignment trends were also observed for 3D striated structures designed to mimic collagen fibers. A fluorescent image

of HFF fixed on the 100 nm cross-striated samples is seen in Fig. 5. Cellular alignment was within experimental error in the presence of 100 nm cross-striations (93.4%) and in the absence of cross-striations (91.7%). Thus, no effect on cell elongation or alignment can be conclusively discerned.

4. Discussion

Contact guidance has long been recognized as a driving force behind topography-directed alignment of cells [15,18,19,42]. This theory relates cell alignment to the probability that a cell will make a successful protrusion in a given direction, based on the features it encounters. For instance, Clark and co-workers [43] characterized the behavior of BHK cells at single step interfaces. They concluded that, due to limited flexibility of the cytoskeleton, cells are unable to frequently traverse significant steps. This limitation was especially prevalent in cells approaching from the lower surface. As a result, polarization and alignment are more likely to occur in the direction

without obstacle, as opposed to the direction of a significant step. Thus, taller steps and decreased pitches (or linewidths) create geometrical barriers with sharp turns and angles that tax the flexibility of the cytoskeleton. These ideas are illustrated in Fig. 4b and c, displaying the average cell widths as a function of linewidth and depth. For a fixed linewidth of 5 μm, the cell width shrinks for increasing depths. Likewise, for a fixed line depth of 100 nm, the cell width decreases for decreasing linewidth. As a result, alignment increases as the cell spreading occurs only in the direction of the lines, both in the trenches and on the ridges. As the line pitch is further reduced to the submicron range, direct bridging over the trenches might account for increased lateral spreading and a decrease in cell alignment, as found for the 100 nm wide lines.

Past studies that measured cell alignment relative to varying linewidths or depths have indeed developed valid relationships between substrate topography and cell morphology; however, the conclusions of different studies in which width and depth are controlled separately rather than one dimension controlled with

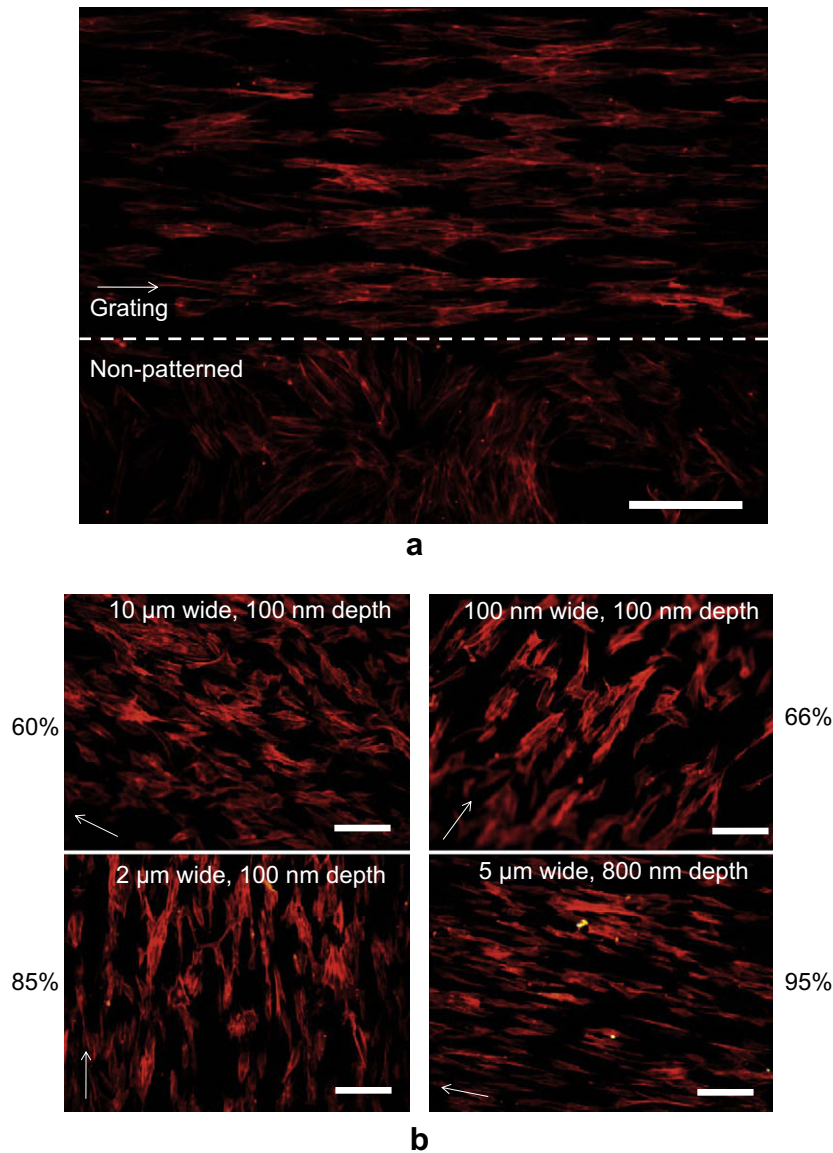


Fig. 2. Fluorescence microscopy images of fibroblasts on various substrates. (a) Cells on patterned grating (2 μm wide, 800 nm deep) and non-patterned areas on the same substrate show very different morphology; (b) cells on lines of 10 μm wide, 100 nm depth; 100 nm wide, 100 nm depth; 2 μm wide, 100 nm depth; and 5 μm wide, 800 nm depth. Arrows indicate the grating direction. Cell alignment percentages are shown beside the images. The scale bar is 30 μm.

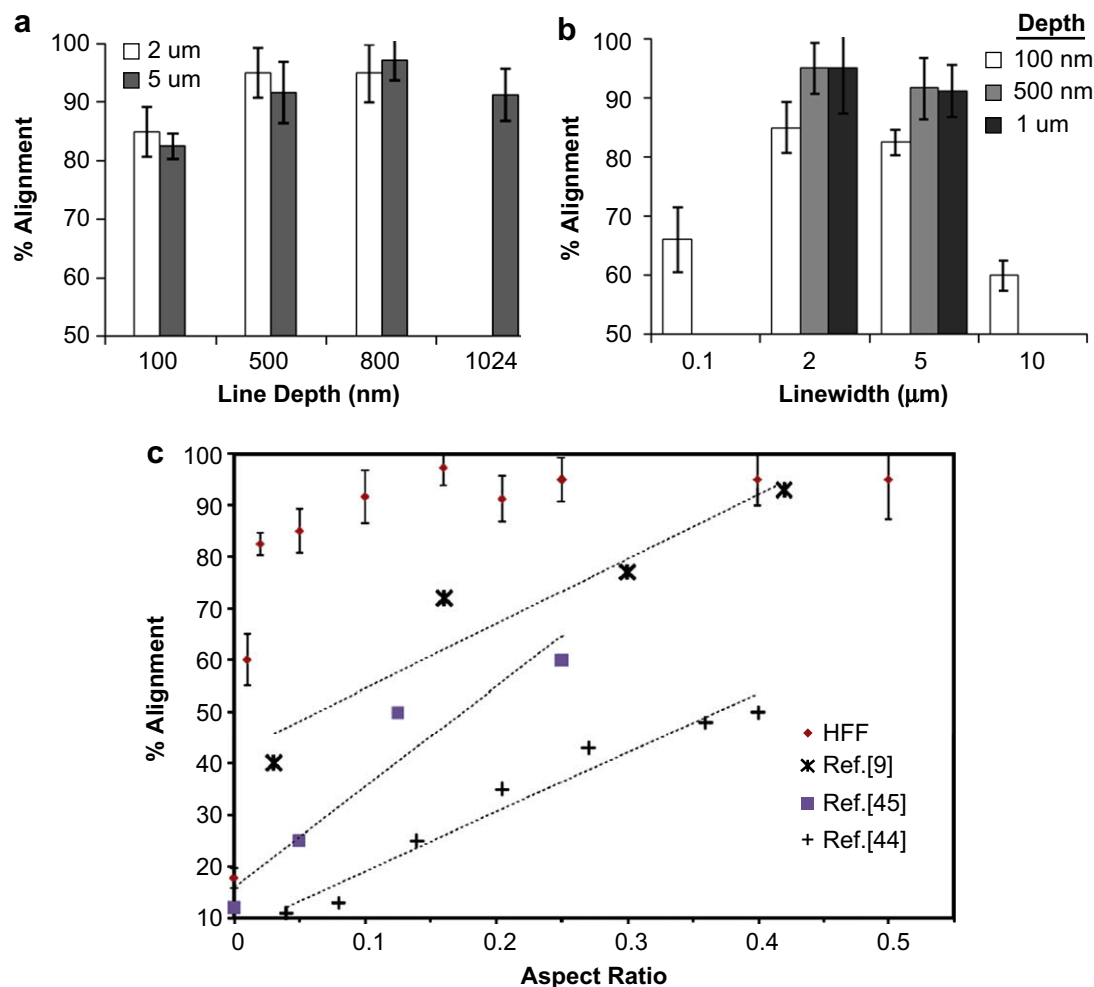


Fig. 3. Cell alignment for various grating dimensions. (a) Alignment vs. depth for 2 and 5 μm wide lines, (b) Alignment vs. linewidth for 100 nm, 500 nm, and 1 μm deep lines, and (c) Alignment vs. aspect ratio for various grating dimensions. Error bars indicate the standard deviation in the mean of the percent alignment on three to five replicate samples of each imprint pattern. Cell alignment results from some previous works are recalculated and then plotted with grating aspect ratio for comparison.

respect to the other are not mutually consistent. For example, the previous study of Hu et al. [9] observed that cell alignment and elongation dramatically increase with decreasing grating pitch from microscale to nanoscale as the depth was kept constant, leading to the conclusion that nanostructures are more effective in guiding cells, while others observed the opposite or different effects of similar topography on cell morphology [3,20], including this study where microstructures are more effective than nanostructures. Such contradictions illustrate the challenge of predicting cell behaviors in response to topographical changes in a single substrate dimension, even when keeping the other dimensions constant. On the other hand, if the cell behaviors are studied as a function of the ratio of the groove depth to width, effects of both dimensions are considered in tandem. As shown in Fig. 3c, for samples varying both the linewidth and depth, we found that across all dimensions within the 1–10 μm range, the aspect ratio described the observed alignment trends. When the aspect ratio is higher than a critical value (only ~ 0.05 in this study), high cell alignment ($>80\%$) can be obtained for a wide range of topographic dimensions, and the effect of the grating depth or width alone on the cell alignment is diminished.

To test the generality of this aspect ratio dependence, cell alignment and elongation measurements from our previous study [9] and also from other groups [44,45] are re-plotted against

structural aspect ratio in Fig. 3c (alignment) and Fig. 4a (elongation). Despite large differences in cell types, culture conditions, structural dimensions, and materials used in these studies, a similar monotonic dependence of cell alignment and elongation on aspect ratio is observed in each case. Notably, there are significant differences in the extent of alignment at similar aspect ratios among these studies. These differences may be due to the use of different cell types, with potentially different sensitivities to similar surfaces, and also to different definitions of alignment. For example, this study (using HFF cells) and previous work (using smooth muscle cells) [9] counted cells as aligned if the angle of their long axis with respect to the grating direction is $\pm 15^\circ$; while Uttayarat et al. [45] and Fraser et al. [44] used endothelial cells with alignment angle of $\pm 20^\circ$, and HCEC cells with alignment angle of $\pm 10^\circ$. Several other studies were also re-plotted, yielding a similar trend and slope in each case (data not shown) [14,19,24,46,47].

These consistent observations suggest that the aspect ratio of topographic features provides a more comprehensive characterization of their effects on cell morphology and alignment than the parameter of a single dimension. Considered another way, an observed cell morphology, such as elongation, plotted vs. parameters of grating width and depth, defines a three-dimensional surface. Variation of a single topographical dimension while holding the other constant, the conventional approach to exploring

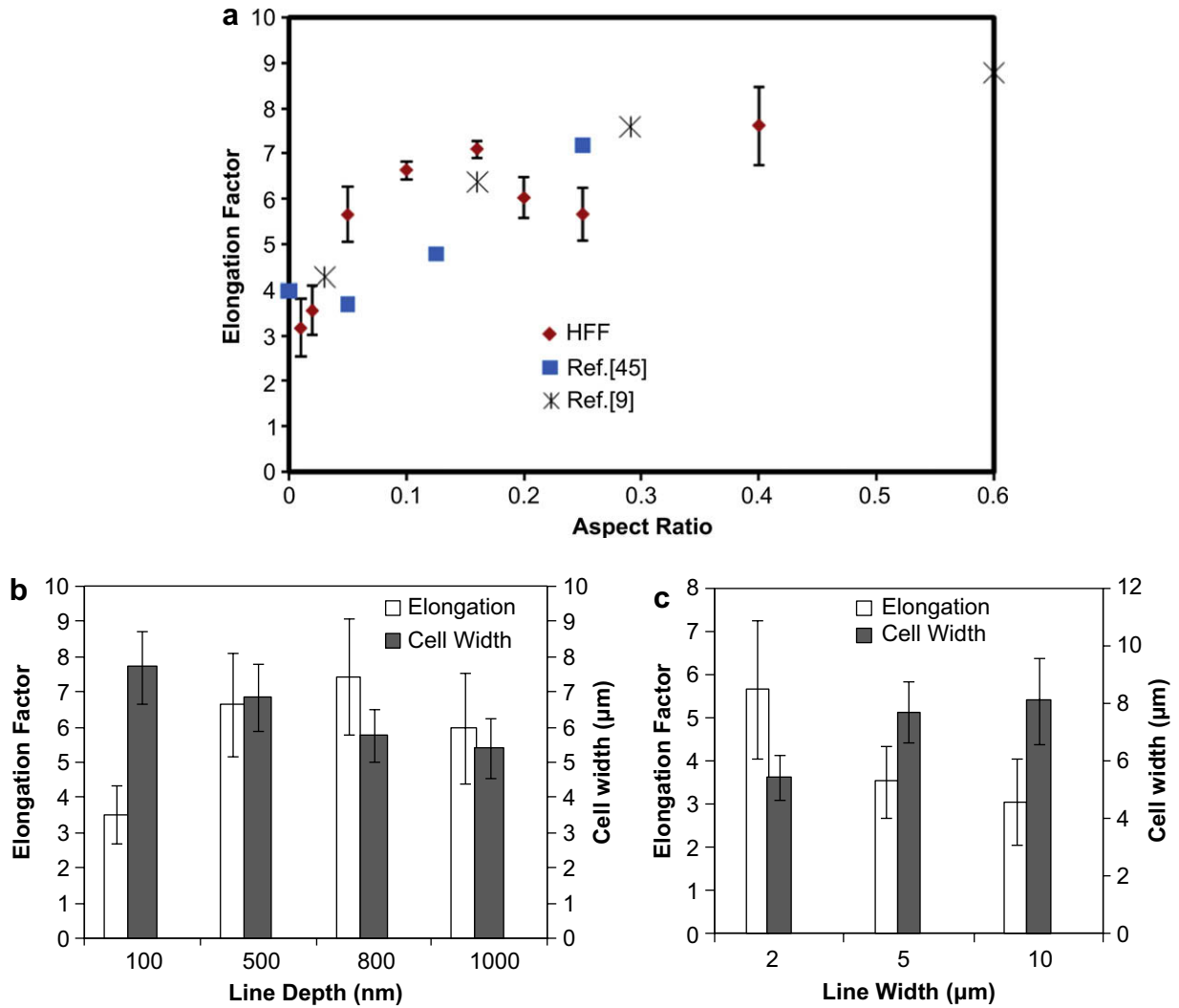


Fig. 4. Elongation vs. (a) aspect ratio, (b) line depth for a fixed 5 μm linewidth, (c) and pitch for a fixed line depth of 100 nm. Note figures (b) and (c) also display the cell width as a function of linewidth and depth. Error bar indicates the standard deviation in the mean of the average values measured on each of three to five replicate samples of imprint pattern. In addition, cell elongation results from some previous works are recalculated and then plotted with grating aspect ratio for comparison in (a).

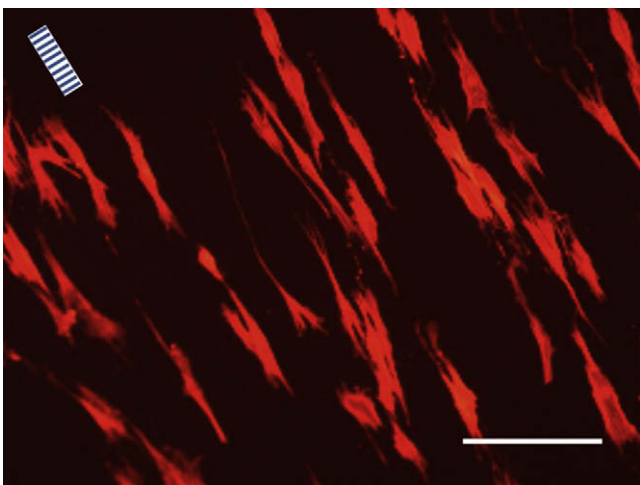


Fig. 5. Fluorescence microscopy image of fibroblasts on double-imprinted structure consisting of 100 nm wide, 60 nm deep lines embedded within 5 μm wide, 500 nm deep lines. Lines in the top left corner indicate the direction of gratings. Scale bar is 30 μm.

effects of gratings, provides only a cross-section of this surface and does not allow prediction of other points on the surface with similar cell behavior. In contrast, feature aspect ratio provides a general relationship that can be applied predicatively to a large variety of width and depth combinations. Because the aspect ratio dependence is a general relationship, a desired cell alignment or elongation can be achieved simply by maintaining an appropriate aspect ratio range, and there are an array of possible combinations of grating width and depth capable of achieving the same results. The simplicity and design flexibility offered by aspect ratio can be useful in the design of tissue scaffolds, medical implants, or even prostheses, where surface preparations are key factors in controlling cell adhesion and morphology.

The theory of cell contact guidance provides a rationale for the observed dependence of anisotropic cell behaviors (alignment and elongation) on topographic aspect ratio. As cells spread on a surface, they extend filopodia to explore their surroundings, forming local adhesions where space and cell adhesion factors are encountered. According to the theory of contact guidance [15,19], cell alignment and elongation are related to the probability that a cell will make a successful protrusion in a given direction. Due to

limited flexibility of the cytoskeleton, steps on the surface present an impediment to spreading [14,43]. On the flat surfaces of ridges (or on the flat surfaces at the bottom of the grooves), the probability for a cell to make a successful protrusion in the direction of the ridge is essentially independent of the grating topography, because it encounters no obstacles when spreading in that direction. Thus, the elongation of the cell along the ridges and the probability of cell alignment with the ridges are inversely related to the probability that it will successfully form a protrusion in the direction perpendicular to the grating.

Wider ridges (and correspondingly wider grooves) allow cells to spread further without encountering a step and also allow the cells to conform to the surface across steps with less severe cytoskeletal bending, both effects increasing the probability of lateral spreading. Deepening the grating without widening the ridges increases the extent of cytoskeletal bending required for a cell to conform to the surface and imposes a stronger impediment on lateral spreading. On the other hand, a corresponding increase in the grating width in conjunction with increased depth relaxes the requirement for cytoskeletal bending and thus diminishes the impediment to lateral spreading. Described another way, for grating dimensions smaller than the cell width, the impediment to lateral spreading is related to the slope of the bend the cell must make to conform to the surface, which is equal to the aspect ratio of the grating. Thus, though the grating dimensions of width and depth can be varied independently, they do not affect the cell spreading and alignment independently but as their ratio.

It is important to point out that this model is valid only for a specific range of dimensions relative to the cell size. When the grating surface is wider than or close to the un-bounded cell width, cell spreading can proceed in the lateral direction largely unimpeded, and the depth of the grooves will have little effect on the cells. Therefore the upper bound of gratings for guided cell alignment is the size of the cell itself. Notably, most studies have used sub-cellular dimensions for their topographic design. At the other extreme, when the grooves are extremely narrow, the cells can easily bridge the gap to neighboring ridges [15]. In this case, even a high aspect ratio (groove is deep relative to width) has a small effect on alignment. For example, sample #11 in Table 1 (100 nm line of 100 nm depth) has the highest aspect ratio tested in this study (equal to 1) but shows only 66% alignment, much lower than smaller aspect ratios on micro-gratings. The lack of an effect for superimposing a nanometer-scale pattern on the micron-scale grating in the double-imprinted samples is also consistent with this limitation. The alignment and elongation measurements yielded results similar to the same micro-gratings without the nano-structure.

Despite these limitations on the relevant scale of topographic features, HFF are sensitive to even the shallowest (100 nm deep) lines tested, confirming the sensitivity of human cells to features well beneath 1 μm . Although alignment appears to be relatively poor on the 100 nm wide, 100 nm deep lines, increased alignment was observed on this surface relative to cells seeded on flat control surfaces. Previous studies of cell behavior in response to nano-topography have yielded similar results. In trying to determine the lower dimensional limit for cell sensitivity, rat dermal fibroblasts were seeded on various nanogrooves. It was concluded that for groove depths as shallow as 35 nm and ridges less than 100 nm in width, the fibroblasts did not show noticeable alignment [10]. Additional studies with corneal epithelial cells have shown only 35% alignment on lines of 70 nm width and 400 nm pitch [34]. While the HFF aligned on the 100 nm lines at a much lower rate than on the micron grooves, 66% alignment is significant relative to other nanoscale studies. While it is difficult to extend the analysis of one study to another of a different cell type, these

results do suggest that HFF might be more sensitive to nanostructures than at least some other mammalian cell types. Other groups have also reported various cell responses and behaviors in the presence of nanostructures, including increased cell proliferation, improved cytoskeletal organization, and overall increased cellular functionalization [17]. These findings confirm the importance of incorporating and utilizing nanostructures in scaffolds and devices to be used in intimate contact with fibroblasts.

5. Conclusion

The flexibility of nanoimprint lithography has enabled us to produce a wide variety of patterns over large areas in TCPs. Gratings of various pitches and depths were utilized to study the effects of the aspect ratio on cell alignment and elongation. Double imprinting was also utilized to create 3D collagen-like structures combining micron and nanostructures. Human dermal fibroblasts were found to increase their alignment and elongation with increasing aspect ratios. While aspect ratios as small as 0.01 induced significant alignment (60%), the maximum aspect ratio required for 95% alignment was 0.16. This study indicates that, within an appropriate range of sizes, the aspect ratio of the topography characterizes the combined effects of pattern width and depth on cell behaviors. Recently published results by other groups were re-plotted with respect to aspect ratio, and the results show a dependence similar to that found in our studies, despite differences in cell types, culture conditions, and structure variation. This correlation indicates that aspect ratio is a generally useful factor to describe cell behaviors, leading to consistent conclusions for various studies and an approach for predicting results for novel combinations of width and depth. A model based on the theory of contact guidance is proposed to explain the dependence of anisotropic cell behaviors on the aspect ratio of surface topography. This model, in conjunction with our data, suggests the range of dimensions for which the relationship between cell aspect ratio and alignment or elongation is valid. These findings provide simplicity and flexibility of topography design for future biomedical applications.

Acknowledgements

The authors would like to thank Professor Chris Wilkinson at the University of Glasgow, UK for useful discussions. This work is supported by the Texas Higher Education Coordinating Board through Advanced Research Program under Contract No. 009741-0015-2006.

Appendix

Figures with essential colour discrimination. Certain figures in this article, in particular Figures 2 and 5 are difficult to interpret in black and white. The full colour images can be found in the on-line version, at doi:10.1016/j.biomaterials.2008.11.041.

References

- [1] Gadegaard N, Mosler S, Larsen N. Biomimetic polymer nanostructures by injection molding. *Macromolecular Materials and Engineering* 2003;288(1): 76–83.
- [2] Curtis A, Gadegaard N, Dalby M, Riehle M, Wilkinson C, Aitchison G. Cells react to nanoscale order and symmetry in their surroundings. *IEEE Transactions on Nanobioscience* 2004;3(1):61–5.
- [3] Eliason M, Charest J, Simmons B, Garcia A, King W. Nanoimprint fabrication of polymer cell substrates with combined microscale and nanoscale topography. *Journal of Vacuum Science and Technology B* 2007;25(4):L31–4.

- [4] Teixeira A, Abrams G, Murphy C, Nealey P. Cell behavior on lithographically defined nanostructured substrates. *Journal of Vacuum Science and Technology B* 2003;21(2):683–7.
- [5] Yim E, Reano R, Pang S, Yee A, Chen C, Leong K. Nanopattern-induced changes in morphology and motility of smooth muscle cells. *Biomaterials* 2005;26(26):5405–13.
- [6] Andersson A, Backhed F, Euler Av, Richter-Dahlfors A, Sutherland D, Kasemo B. Nanoscale features influence epithelial cell morphology and cytokine production. *Biomaterials* 2003;24:3427–36.
- [7] Charest J, Bryant L, Garcia A, King W. Hot embossing for micropatterned cell substrates. *Biomaterials* 2004;25:4767–75.
- [8] Dalby M, Riehle M, Sutherland D, Agheli H, Curtis A. Changes in fibroblast morphology. *Biomaterials* 2004;25:5415–22.
- [9] Hu W, Yim E, Reano R, Leong K, Pang SW. Effects of nanoimprinted patterns in tissue-culture polystyrene on cell behavior. *Journal of Vacuum Science and Technology* 2005;23(6).
- [10] Loesberg W, Riet J, Delft Fv, Schon P, Figdor C, Speller S, et al. The threshold at which substrate nanogroove dimensions may influence fibroblast alignment and adhesion. *Biomaterials* 2007;28:3944–51.
- [11] Luebke K, Carter D, Garner H, Brown K. Patterning adhesion of mammalian cells with visible light, tris(bipyridyl)ruthenium(II) chloride, and a digital micromirror array. *Journal of Biomedical Materials Research Part A* 2004;68A(4):696–703.
- [12] Berry C, Curtis A, Oreffo R, Agheli H, Sutherland D. Human fibroblast and human bone marrow cell response to lithographically nanopatterned adhesive domains on protein rejecting substrates. *IEEE Transactions on Nanobioscience* 2007;6(3):201–9.
- [13] Lenhert S, Meier M, Meyer U, Chi L, Wiesmann H. Osteoblast alignment, elongation and migration on grooved polystyrene surfaces patterned by Langmuir–Blodgett lithography. *Biomaterials* 2005;26:563–70.
- [14] Clark P, Connolly P, Curtis A, Dow J, Wilkinson C. Topographical control of cell behaviour: II. Multiple grooved substrate. *Development* 1990;108:635–44.
- [15] Curtis A, Wilkinson C. Topographical control of cells. *Biomaterials* 1997;18:1573–83.
- [16] Flemming RG, Murphy CJ, Abrams GA, Goodman SL, Nealey PF. Effects of synthetic micro- and nano-structured surfaces on cell behavior. *Biomaterials* 1999;20:573–88.
- [17] Sniadecki N, Desai R, Ruiz S, Chen C. Nanotechnology for cell–substrate interactions. *Annals of Biomedical Engineering* 2006;34(1):59–74.
- [18] Weiss P. Experiments on cell and axon orientation in vitro: the role of colloidal exudates in tissue organization. *Journal of Experimental Zoology* 1945;100:353–86.
- [19] Clark P, Connolly P, Curtis A, Dow J, Wilkinson C. Cell guidance by ultrafine topography in vitro. *Journal of Cell Science* 1991;99:73–7.
- [20] Wojciakstothard B, Madeja Z, Korohoda W, Curtis A, Wilkinson C. Activation of macrophage-like cells by multiple grooved substrata – topographical control of cell behavior. *Cell Biology International* June 1995;19(6):485–90.
- [21] Ponnsoneta L, Comteb V, Othmanec A, Lagneaub C, Charbonnierd M, Lissacb M, et al. Effect of surface topography and chemistry on adhesion, orientation and growth of fibroblasts on nickel–titanium substrates. *Materials Science and Engineering C* 2002;21(1–2):157–65.
- [22] Anselme K, Bigerelle M, Noël B, Iost A, Hardouin P. Effect of grooved titanium substratum on human osteoblastic cell growth. *Journal of Biomedical Materials Research Part A* 2002;60(4):529–40.
- [23] Ball M, Grant DM, Lo W-J, Scotchford CA. The effect of different surface morphology and roughness on osteoblast-like cells. *Journal of Biomedical Materials Research Part A* 2008;86(3):637–47.
- [24] Lenhert S, Sesma A, Hirtz M, Chi L, Fuchs H, Wiesmann HP, et al. Capillary-induced contact guidance. *Langmuir* 2007;23(20):10216–23.
- [25] Kane R, Takayama S, Ostuni E, Ingber D, Whitesides G. Patterning proteins and cells using soft lithography. *Biomaterials* 1999;20:2363–76.
- [26] Jackman R, Wilbur J, Whitesides G. Fabrication of submicrometer features on curved substrates by microcontact printing. *Science* 1995;269(5224):664–6.
- [27] Hahn M, Taite L, Moon J, Rowland M, Ruffino K, West J. Photolithographic patterning of polyethylene glycol hydrogels. *Biomaterials* 2006;27(12):2519–24.
- [28] Stevens M, George J. Exploring and engineering the cell surface interface. *Science* 2005;310:1135–8.
- [29] Ishaug-Riley S, Crane-Kruger G, Yaszemski M, Mikos A. Three-dimensional culture of rat calvarial osteoblasts in porous biodegradable polymers. *Biomaterials* 1998;19:1405–12.
- [30] Vozzi G, Previti A, Rossi DD, Ahluwalia A. Microsyringe-based deposition of two-dimensional and three-dimensional polymer scaffolds with a well-defined geometry for application to tissue engineering. *Tissue Engineering* 2002;8(6):1089–98.
- [31] Mooney D, Baldwin D, Suh N, Vacanti J, Langer R. Novel approach to fabricate porous sponges of poly(D,L-lactic-co-glycolic acid) without the use of organic solvents. *Biomaterials* 1996;17:1417–22.
- [32] Deckman H, Dunsmuir J. Natural lithography. *Applied Physics Letters* 1982;41(4):377–8.
- [33] Chew S, Mi R, Hoke A, Leong K. The effect of the alignment of electrospun fibrous scaffolds on Schwann cell maturation. *Biomaterials* 2008;29:653–61.
- [34] Teixeira A, Abrams G, Bertics P, Murphy C, Nealey P. Epithelial contact guidance on well-defined micro- and nanostructured substrates. *Journal of Cell Science* 2003;116(10):1881–92.
- [35] Tan H, Gilbertson A, Chou S. Roller nanoimprint lithography. *Journal of Vacuum Science and Technology B* 1998;16(6):3926–8.
- [36] Ahn SH, Guo J. High-speed roll-to-roll nanoimprint lithography on flexible plastic substrates. *Advanced Materials* 2008;9999(9999):1–6.
- [37] Chou S, Krauss P, Renstrom P. Imprint lithography with 25-nanometer resolution. *Science* 1996;277:85–7.
- [38] Austin M, Ge H, Wu W, Li M, Yu Z, Wasserman D, et al. Fabrication of 5 nm linewidth and 14 nm pitch features by nanoimprint lithography. *Applied Physics Letters* 2004;84(26):5299–301.
- [39] Guo LJ. Recent progress in nanoimprint technology and its applications. *Journal of Physics D Applied Physics* 2004;37:R123–41.
- [40] Hu W, Yang B, Peng C, Pang SW. Three-dimensional SU-8 structures by reversal UV imprint. *Journal of Vacuum Science and Technology B* 2006;24(5):2225–9.
- [41] Buck E, Petersen K, Hund M, Krausch G, Johannsmann D. Decay kinetics of nanoscale corrugation gratings on polymer surface: evidence for polymer flow below the glass temperature. *Macromolecules* 2004;37(23):8647–52.
- [42] Oakley C, Brunette D. The sequence of alignment of microtubules, focal contacts and actin filaments in fibroblasts spreading on smooth and grooved titanium substrata. *Journal of Cell Science* 1993;106:343–54.
- [43] Clark P, Connolly P, Curtis A, Dow J, Wilkinson C. Topographical control of cell behaviour: I. Simple step cues. *Development* 1987;99:439–48.
- [44] Fraser S, Ting Y, Mallon K, Wendt A, Murphy C, Nealey PF. Sub-micron and nanoscale feature depth modulates alignment of stromal fibroblasts and corneal epithelial cells in serum-rich and serum-free media. *Journal of Biomedical Materials Research Part A* 2008;86(3):725–35.
- [45] Uttayarat P, Toworfe GK, Dietrich F, Lelkes PI, Composto RJ. Topographic guidance of endothelial cells on silicone surfaces with micro- to nanogrooves: orientation of actin filaments and focal adhesions. *Journal of Biomedical Materials Research Part A* 2005;75A(3):668–80.
- [46] Charest JL, Garcia AJ, King WP. Myoblast alignment and differentiation on cell culture substrates with microscale topography and model chemistries. *Biomaterials* April 2007;28(13):2202–10.
- [47] denBraber ET, deRuijter JE, Ginsel LA, vonRecum AF, Jansen JA. Quantitative analysis of fibroblast morphology on microgrooved surfaces with various groove and ridge dimensions. *Biomaterials* Nov 1996;17(21):2037–44.